Proceedings Paper:

Bogosian, D., Rigby, S.E. and Powell, D. (2016) A comprehensive comparison of methods for clearing effects on reflected airblast impulse. In: Proceedings of the 24th Military Aspects of Blast and Shock. 24th Military Aspects of Blast and Shock, 19-23 Sep 2016, Halifax, Nova Scotia, Canada. MABS .

A COMPREHENSIVE COMPARISON OF METHODS FOR CLEARING EFFECTS ON REFLECTED AIRBLAST IMPULSE

D. Bogosian[1], S. Rigby[2] D. Powell[1]

[1]Baker Engineering and Risk Consultants,
360 N. Sepulveda Blvd., Ste 1090, El Segundo, CA 90245, USA;
[2]University of Sheffield, Department of Civil & Structural Engineering,
Sir Frederick Mappin Building, Mappin Street, Sheffield, S1 3JD, United Kingdom

ABSTRACT

Having calculated the free-field pressure history at the location of a building, an engineer engaged in design or assessment of that building must then calculate the loads on the various surfaces of the structure. Numerous engineering methods have been developed that provide approximate (and generally conservative) approaches towards the calculation of these loads. Of greatest importance is the load on the front face (i.e., the building surface directly facing the explosion source). Depending on the size of the building and the blast load duration, clearing effects due to the building's boundaries may reduce the reflected impulse on the front face from the fully reflected value predicted by standard blast models.

Unfortunately, there are many methods available in the literature for evaluating clearing effects, each using somewhat similar, yet distinctly different, equations. One approach given in UFC 3-340-02 (and reproduced in UFC 3-340-01) has gained widespread acceptance; another is presented in a set of guidelines published by ASCE and used for industrial applications; and lastly, a formerly classified study dating back to 1955 which, although declassified in 1998, seems to have escaped the notice of the blast community.

The focus of the present paper is to evaluate all three of these methods empirically, by comparing their results against a series of blast tests with varying charge weights and scaled reflecting building dimensions. A comparative evaluation is then made of the strengths and weaknesses of each approach, with recommendations for future use by researchers and blast engineers.

INTRODUCTION

Obtaining the blast load to be used in design or assessment of a building nearly always involves the calculation of the reflected loading on the building surface facing the explosion source. The applied loading on the facing surface deviates from the nominal free-field pressure history in at least three ways: (1) the peak pressure is reflected to a higher value than the free-field; (2) the pressure history may be affected by clearing effects due to the finite size of the reflecting surface; and (3) the addition of a dynamic (drag) pressure component to the overall loading. This paper deals with the second of those phenomena, clearing effects, and evaluates three different approaches that are available to blast engineers for computing those effects. Our purpose is to demonstrate the shortcomings of the methods commonly seen in the literature for calculating clearing effects, and to promote the use of a more physical and better validated approach that has yet to gain widespread acceptance.

PHYSICS OF CLEARING EFFECTS

The most commonly used standard model for airblast parameters is the set of curves originally developed by Kingery and Bulmash [1] for hemispheres of TNT at ground surface (as well as for spheres of TNT in free air). These curves have been incorporated in numerous publications, including government design manuals such as UFC 3-340-02 [2]. Curves are provided for both free-field and reflected pressure and impulse. However, this fully reflected impulse is applicable only to cases where the reflector is of infinite size and there are no attenuating effects perceptible at the location of interest from the edges of the loaded surface. This can be a reasonable approximation, but in many cases, particularly where the blast load is of long duration or the reflecting surface is of relatively small size, clearing effects become important.

In basic terms, as a shock wave from a surface burst travels through the air, at a sufficient distance from the source it essentially becomes a planar shock front. For the purposes of this paper, we will assume that the wave then interacts with a wall that is (*a*) rigid and (*b*) orthogonal to the direction of wave propagation. At that point, a reflection is generated and propagated back towards the explosion source. If this reflecting surface is infinite, the reflected pressure and impulse parameters provided by Kingery-Bulmash can be used to calculate the pressure history experienced by a gauge mounted in that wall.

However, if the wall is of finite size, a rarefaction or clearing wave (of negative magnitude) will begin to propagate from the edges of the wall towards the location of the gauge, as shown in Figure 1. As soon as this wave reaches the gauge location, the pressure history no longer conforms to the case of the infinite reflector and the pressure will be somewhat reduced. Note that for shock waves, clearing does not impact the peak pressure, but only the impulse.[1] Note as well that if the clearing wave arrives *after* the positive phase terminates, then clearing effects need not be considered (i.e., no positive phase impulse reduction will occur). Clearing is therefore of interest only when the blast wave duration is long, and/or the reflecting surface is small, in relative terms.

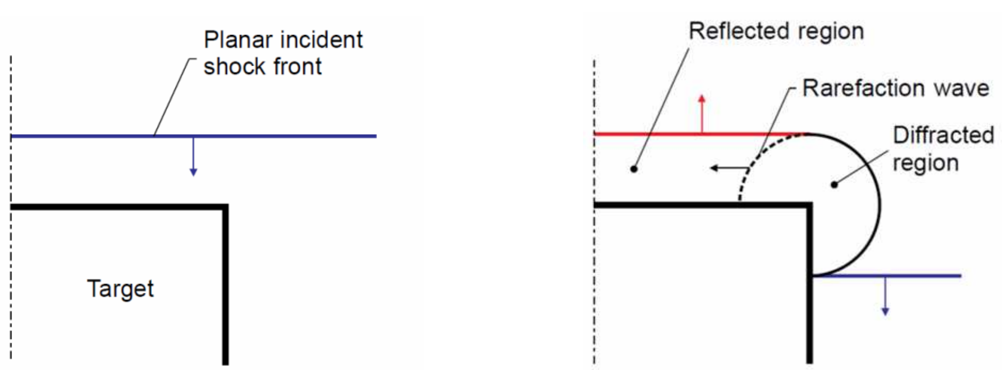

Figure 1: Illustration of rarefaction (clearing) wave propagation.

Neglecting clearing effects is conservative for the purposes of design (i.e., inclusion of clearing effects will reduce the impulse from the value provided by Kingery-Bulmash). This level of

[1] In the more generic case of a pressure wave with a finite rise time, such as those produced by vapour cloud explosions, clearing could also affect the peak pressure. The present paper limits its discussion to shock waves from high explosives such as TNT.

conservatism is often acceptable and the added effort required for calculating clearing effects is not justified. However, when a more refined answer is needed or is beneficial to the project, inclusion of clearing effects is a valuable tool in the designer's arsenal.

TRADITIONAL APPROACHES TO CLEARING

Two methodologies are presented in this section from the published literature for calculating an applied blast pressure history on a surface facing an explosion source while accounting for clearing effects. These are the methods presented in UFC 3-340-02 [2], which is widely used in anti-terrorist design as well as explosive safety, and ASCE [3], which is widely used for designing facilities to resist blast from vapor cloud explosions.

A third approach is the undocumented approach incorporated into the widely used software ConWep [4], but this method was already reviewed and dismissed as inaccurate in earlier work [5] and will not be considered here.

UFC 3-340-02 Approach to Clearing

The approach presented in UFC 3-340-02 is summarized in Figure 2.[2] The user first obtains, from the Kingery-Bulmash curves, a waveform of free-field pressure characterized by the peak pressure p_{so} and duration t_{of}. Note that, as a simplification, the standard exponentially decaying pressure waveform has been replaced with a triangle with duration equal to $2i_s/p_{so}$ where i_s is the free-field impulse. The user then obtains the peak reflected pressure, p_r, also from the Kingery-Bulmash curves.

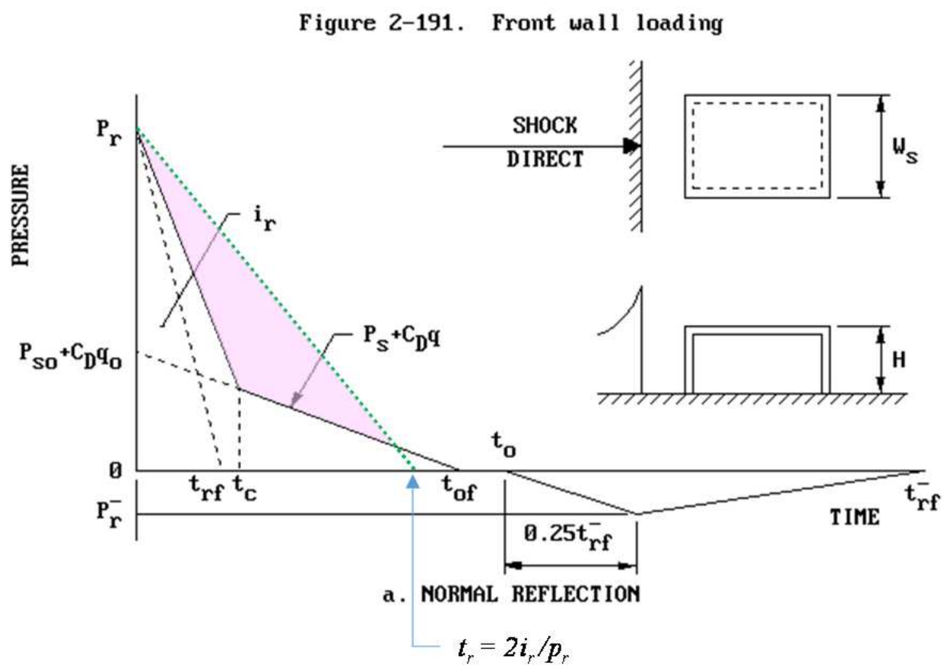

Figure 2: Illustration of clearing methodology in UFC 3-340-02 (from [2], with edits).

[2] Note that in our discussion, we will assume the dynamic or drag pressure contribution to the loading is minimal and can be ignored.

Next, the user calculates a clearing time t_c, which is obtained from the following equation:

$$t_c = \frac{4S}{(1+R)C_r} \tag{1}$$

where

$S = \min\{H, W/2\}$, effectively the distance to the nearest free edge

$$R = \frac{S}{\max\{H, W/2\}}$$

C_r = the speed of sound in the reflected region, obtained from a curve

The manual assumes, as a worst case, that the point of interest is at the bottom of the panel, in the middle, as shown in Figure 3. For a simple case in which the reflector is twice as wide as its height (and thus R=1), the clearing time is thus 2(S/C_r), or twice the time for the clearing wave to travel from the free edge to the assumed point of interest. If the building becomes very wide (i.e., $W >> H$), in the limit, R approaches zero, and the clearing time becomes four times the time required for the clearing wave to travel from the top edge to the bottom.

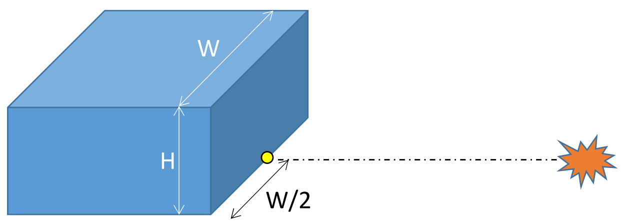

Figure 3: Geometry of reflecting surface and assumed gauge position.

Once the clearing time is calculated, a line segment is drawn from the peak reflected pressure to whatever free-field pressure occurs at the clearing time (neglecting for the time being the drag pressure, which is generally small), after which the free-field pressure applies. This results in the bilinear waveform illustrated in Figure 2.

Were clearing effects to be neglected, and assuming that the duration of the reflected pressure is approximately equal to the duration of the incident pressure, the green dotted line in Figure 2 would represent the applied load. Thus, considering clearing reduces the impulse an amount equal to the area shown on the graph in pink. Depending on the relative magnitude of the clearing time as compared to the reflected duration (t_c as compared to t_r), this reduction can be quite significant, such as when the point in question is very near a free edge.

<u>ASCE Approach to Clearing</u>

The ASCE document takes a very similar approach to clearing, again defining a bilinear waveform constructed out of two triangles with their intersection at the clearing time t_c. However, the ASCE method eschews the complexities resulting from the building's aspect ratio, which, as we saw before, result in a factor of 2 to 4 being applied to the S/C_r ratio. Instead, the ASCE equation is simply:

$$t_c = \frac{3S}{U} \tag{2}$$

where S is the same as before (the distance to the nearest free edge) and U is an alternate symbol for sound speed. An "average" value of 3 therefore replaces the function whose value ranged from 2 to 4.

Some Observations

Both the UFC and ASCE approaches implicitly assume that clearing begins instantaneously (i.e., that the pressure is reduced from its fully reflected value immediately after arrival). This is clearly not physical, since it takes at least a time of (S/C_r) for the clearing wave to reach the gauge location, during which time there should be no reduction in the pressure history from the fully reflected case.

A more defensible methodology would indicate that the waveform remains unchanged up to the time at which the clearing wave first arrives at the gauge (t_1). There would then be a period of time during which the clearing wave interacts with the reflected wave (t_1 to t_2). At time t_2 those interactions would be over and the pressure would revert to the free-field value. This hypothesis, as applied to the more realistic exponential waveform rather than the triangle, is presented in Figure 4. A similar construction could also be made using triangular rather than exponential waveforms. Note that a simple straight-line segment has been used to connect the two segments in the middle transitional portion, although the behaviour during that interval will likely be more complex.

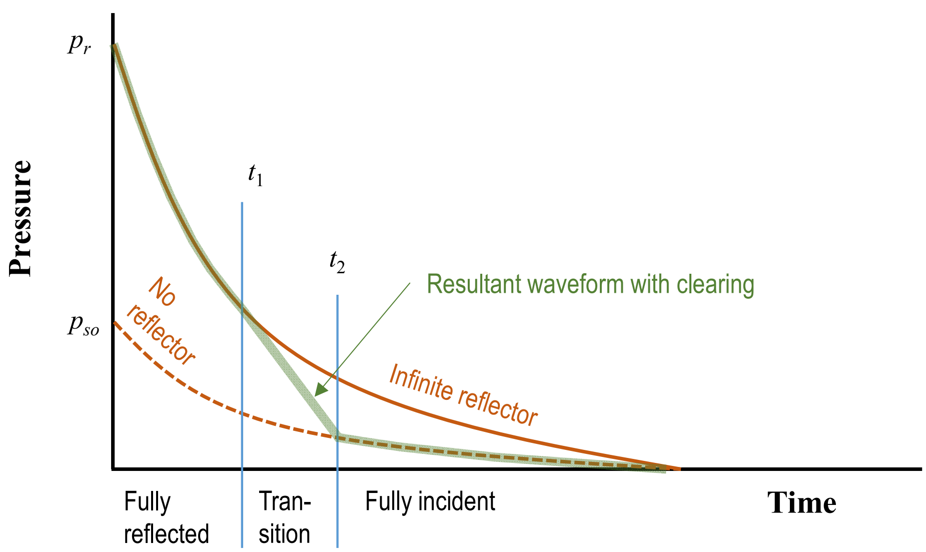

Figure 4: Schematic waveform to represent clearing effects.

A NEW (OLD) METHODOLOGY

In addition to the two manual methods, we present a third method for calculating clearing effects which, though quite old when judged by its actual age, can also be considered very new to most readers because it has not been widely considered or adopted. This procedure, termed the "Hudson method" after its developer C.C. Hudson, originates from a Sandia Corporation Technical Memorandum, first published in 1955 and classified until 1998 [6]. In that document, a map of the spatial and temporal characteristics of the clearing wave was developed analytically, using Sommerfeld diffraction theory and assuming the case of a plane, weak exponential blast wave impinging normally onto a flat, rigid, finite-sized target.

Given the distance from the point of interest to a free edge, the Hudson clearing length, η, can be calculated by dividing this physical length by the 'length' of the positive phase of the blast, using the graphs provided. For weak shocks, this can be approximated by the positive phase duration multiplied by ambient sonic velocity. The dimensionless clearing relief pressure waveform (normalized by the peak incident pressure) can then be estimated as a function of dimensionless time (normalized by the positive phase duration, with clearing length subtracted to account for the arrival time of the clearing wave), using the curves in Figure 5.

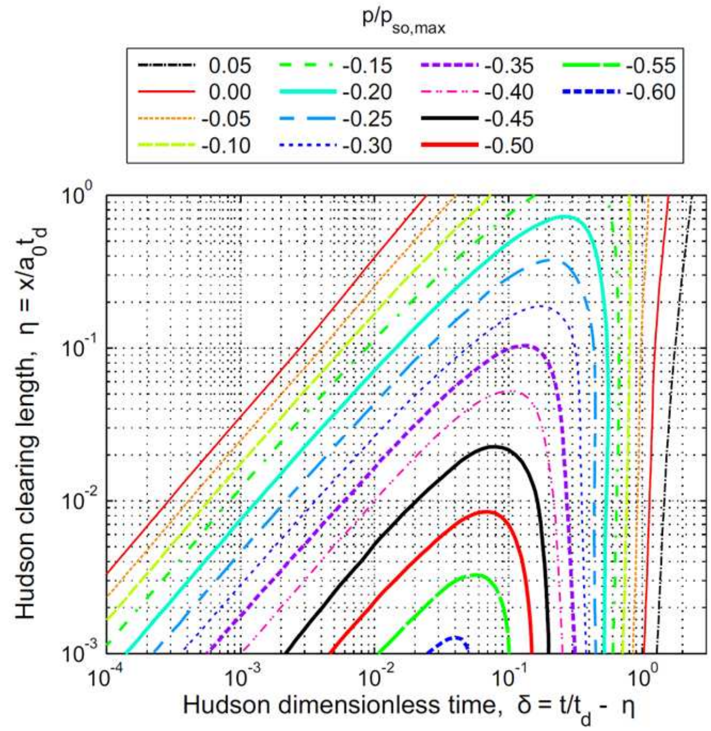

Figure 5: Normalized map of the spatial and temporal characteristics of the relief wave (from [6]).

Each free edge serves as the source of a separate clearing wave. Note that, by applying symmetry to a wall sitting at ground surface, there would be not only clearing waves from the top and side edges, but also from the symmetric free edge at the bottom (below ground), as illustrated in Figure 6. This in effect accounts for the fact that, in the real case, the clearing wave off the top edge would itself be reflected off the ground surface.

Every target would then have to account for four clearing waves, but Hudson allows for an exception: if the distance travelled by the wave from the free edge to the target exceeds that of the free edge, the wave is to be ignored. For example, consider a target at the centroid of a square wall (Figure 7, left). The ray from the top edge travels a length $S_2 < L_1$, and is therefore included. The two rays from the sides travel a length $S_1 < L_2$, and are therefore included. But the ray from the bottom travels $(L_2 - S_2) > L_1$, and is therefore excluded. For a wide, low wall, however, the situation is different (Figure 7, right). Now, the ray from the bottom is included because $(L_2 - S_2) < L_1$, while the rays from the sides are excluded because $S_1 > L_2$.

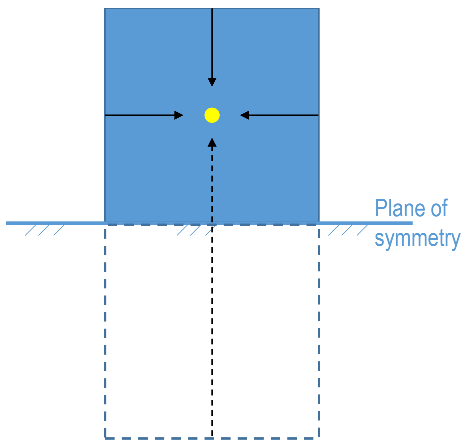

Figure 6: Clearing waves at a target on a wall.

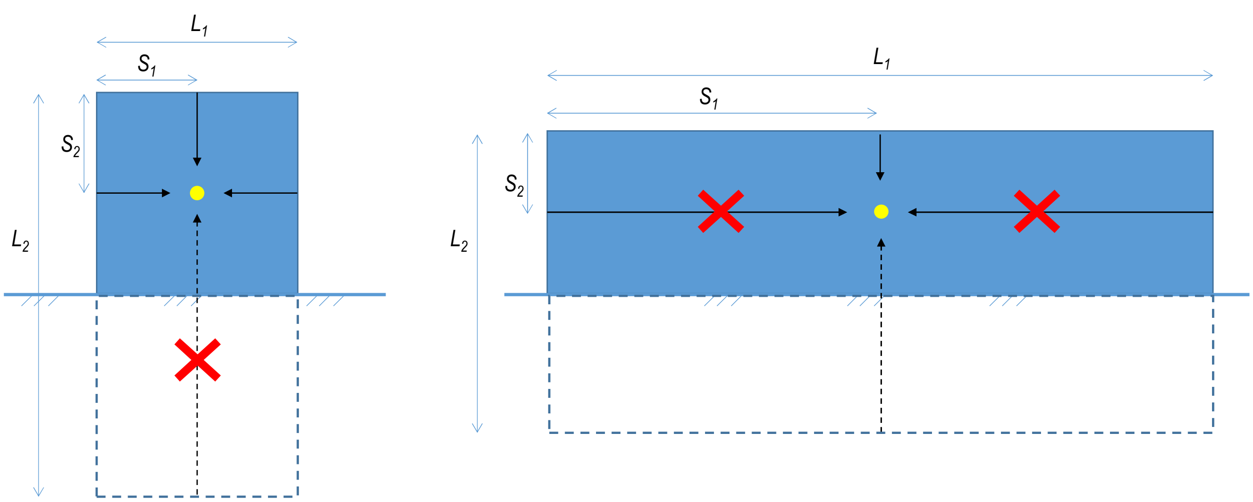

Figure 7: Application of Hudson's rule for omitting individual clearing waves.

For each included ray, a negative pressure history can be calculated using Figure 5. Each of these clearing waves can then be superimposed (through linear addition) with the fully reflected pressure to give a prediction of the cleared blast pressure at that point. For example, for a target at the center of a square wall, the same clearing wave will be multiplied by three and subtracted from the reflected pressure, since all three clearing waves arrive simultaneously. The resulting "scooped" or "scalloped" waveform (Figure 8) is the typical product of this process. If the target were not symmetrically placed relative to the three free edges, two or three separate scallops, each one dropping below the other, would result. Figure 9 shows the process applied to a target where the clearing wave from the top edge arrives first, at t_1, while two additional clearing waves from the sides arrive later, at t_2. The final waveform thus exhibits two scallops.

The Hudson approach has the intrinsic appeal of attempting to remain consistent with the physics of clearing phenomena, and of accounting for each clearing wave (from each free edge) individually. It can thus be applied to any point on a reflecting surface without requiring approximation or further idealisation. It is somewhat more involved numerically than the UFC or ASCE methods, requiring interpolation from among nested curves to determine the clearing waveforms and then superimposing them, but with a computer on the desk (and in the palm) of every engineer, this should not be as a serious obstacle.

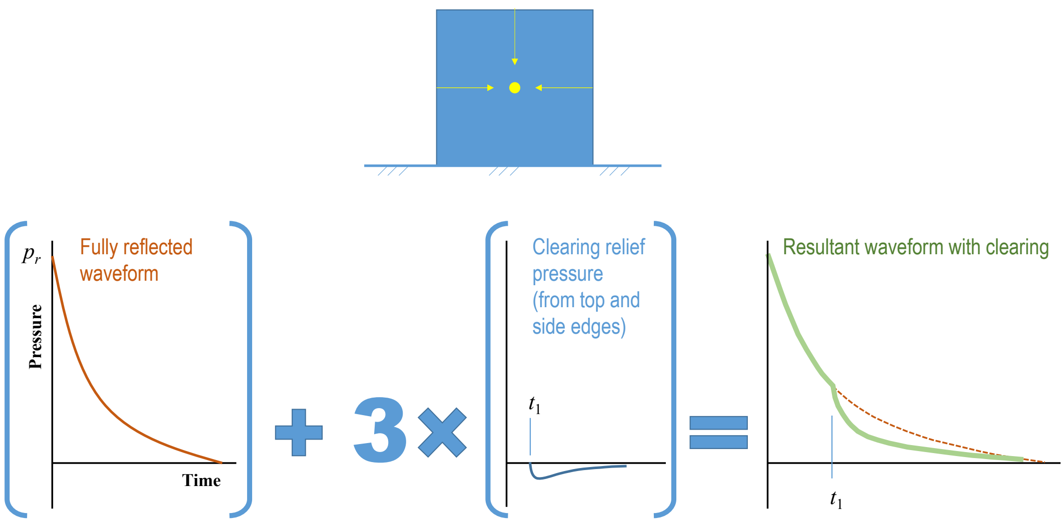

Figure 8: Schematic representation of clearing wave superposition for a target at the center of a square wall.

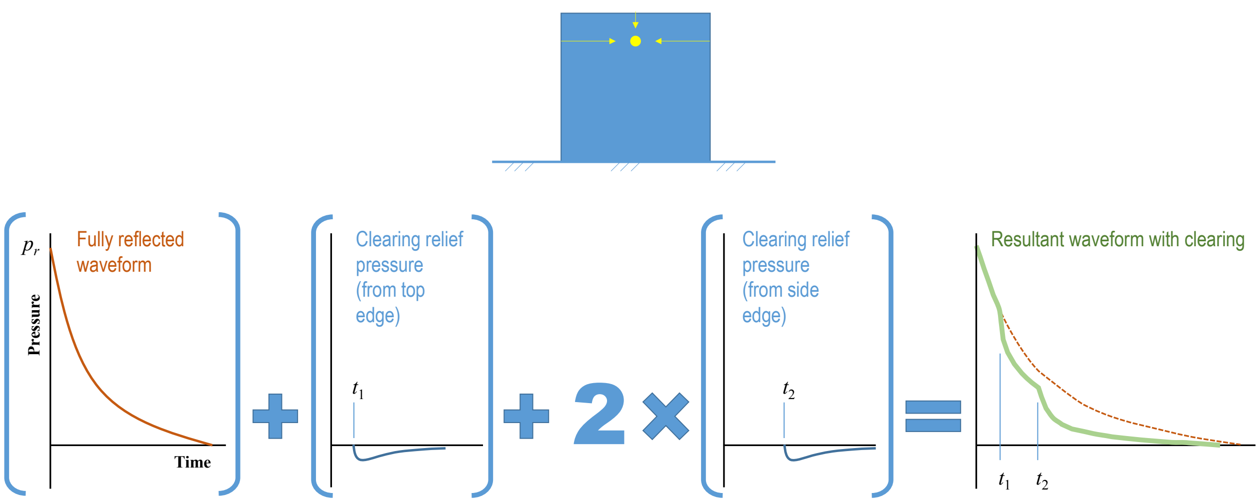

Figure 9: Schematic representation of clearing wave superposition for target near top edge of a wall.

EXPERIMENTAL DATA

A comparison of all three methods with experimental data is required to draw conclusions regarding the relative accuracy of these three approaches. The data came from a series of trials conducted expressly for the purpose of evaluating clearing effects [5]. The tests, schematically illustrated in Figure 10, were simple and designed to match idealized conditions to the extent possible. A hemispherical charge of PE4 (British equivalent of C4) was detonated on the surface of a flat, level concrete slab. A non-responding reinforced concrete block was positioned at some distance from the charge, with the front face having dimensions of 675 mm high by 710 mm (nearly square). The block contained two pressure gauges in its front face, G1 at the geometric centre and G2 halfway to the top free edge. G1 will thus see clearing waves arriving simultaneously from three edges (two sides and top), while G2 will first see the clearing wave from the top followed by the clearing waves from the two sides.

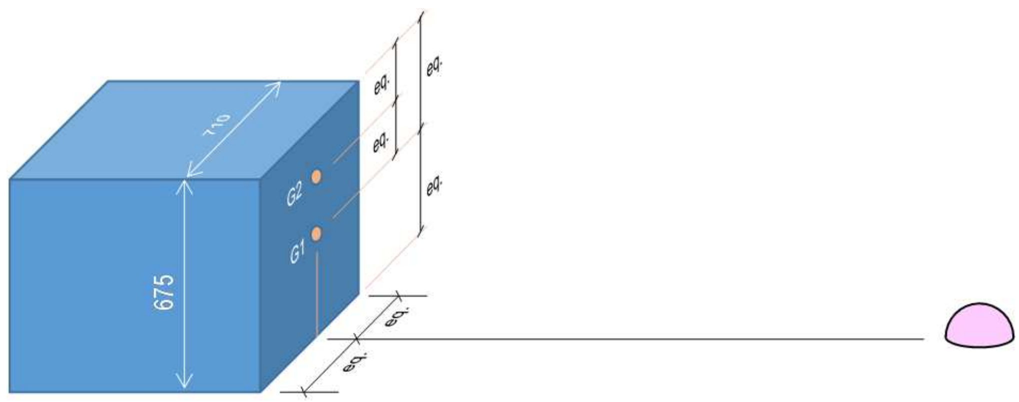

Figure 10: Test setup for validation experiments.

Tests were conducted using 250 g hemispheres of PE4 at standoffs of 4, 6, 8, and 10 m from the front face of the block. In this paper, we will focus exclusively on results from the 4 and 10 m standoff tests, since the phenomenology is identical at the intermediate ranges.

Two tests were conducted for each standoff to demonstrate the repeatability of the measurements. Figure 11 plots pressure histories from the two tests for gauge G1 at a standoff of 4 m, and gauge G2 at 10 m. These are representative of all the gauge records examined, and demonstrate a very high level of repeatability and consistency from test to test. The two test records were therefore averaged to produce a single pressure history for a given standoff and gauge. This averaged history will be shown as the test pressure history for the remainder of this paper.

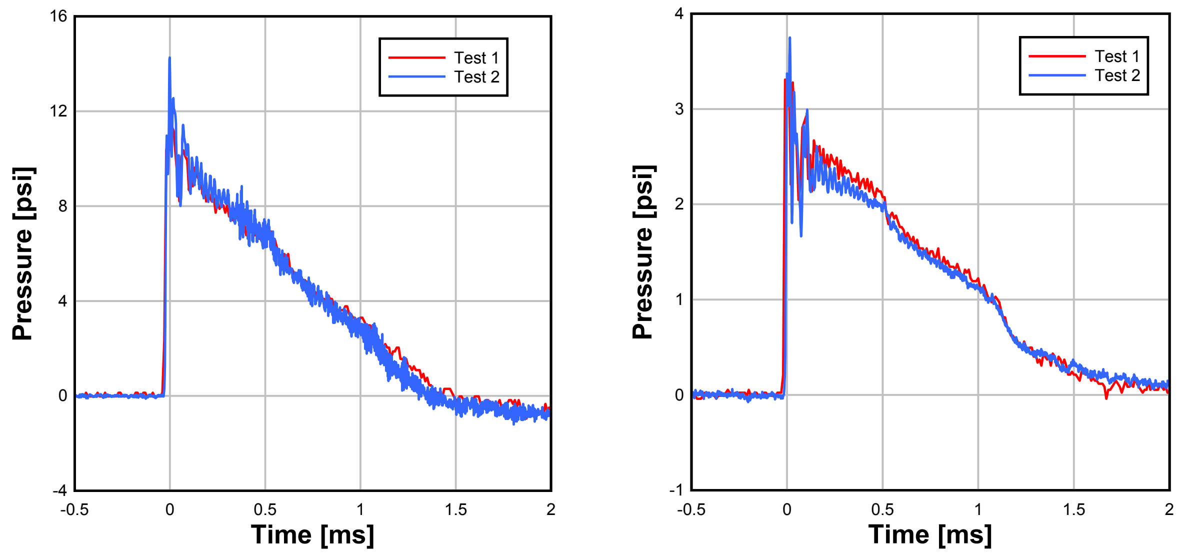

(a) G1 at 4m standoff **(b) G2 at 10m standoff**

Figure 11: Demonstration of repeatability in test data.

COMPARISON OF METHODS

Pressure Waveforms

All three methods were applied towards computation of a pressure history at each of the two gauge locations. For the UFC and ASCE methods, the distance to the nearest free edge and the dimensions of the panel were easily plugged into the appropriate equations to produce the clearing time t_c. In order to remain consistent with the intent of those design manuals, the nominal blast parameters (free-field pressure, impulse, and duration, as well as reflected pressure) were obtained from Conwep using the hemispherical surface burst option, and using a presumed TNT equivalence of 1.2 (i.e., the 250 g of PE4 was converted to 300 g of TNT).

For the Hudson method, G1 is thus analogous to Figure 8, while G2 is similar to Figure 9. Note that for both locations, the fourth wave from the bottom edge (below ground level) is omitted per Hudson's rule set. The clearing lengths from the gauge to the top and side edges were evaluated for each gauge location, and the corresponding clearing functions were superimposed onto the ConWep reflected pressure for 300 g TNT.

Comparison of results at the 4 m standoff is shown in Figure 12. At this close standoff, the waveform duration is relatively short; using the equivalent triangular pulse, it is only about 2.1 ms. At G1 in the centre, ASCE predicts that clearing time exceeds the pulse duration and therefore no clearing effects are expected; UFC's clearing time is only just before the pressure has decayed to zero (at 1.9 ms). Hudson, on the other hand, indicates clearing wave arrival at 1.0 ms, a feature that is clearly visible in the test data at the same point in time. The magnitude of the clearing wave predicted by Hudson (note that here we have three different waves being superimposed, per Figure 8) is somewhat greater than that seen in the data, but the two waveforms are reasonably similar throughout the rest of the history.

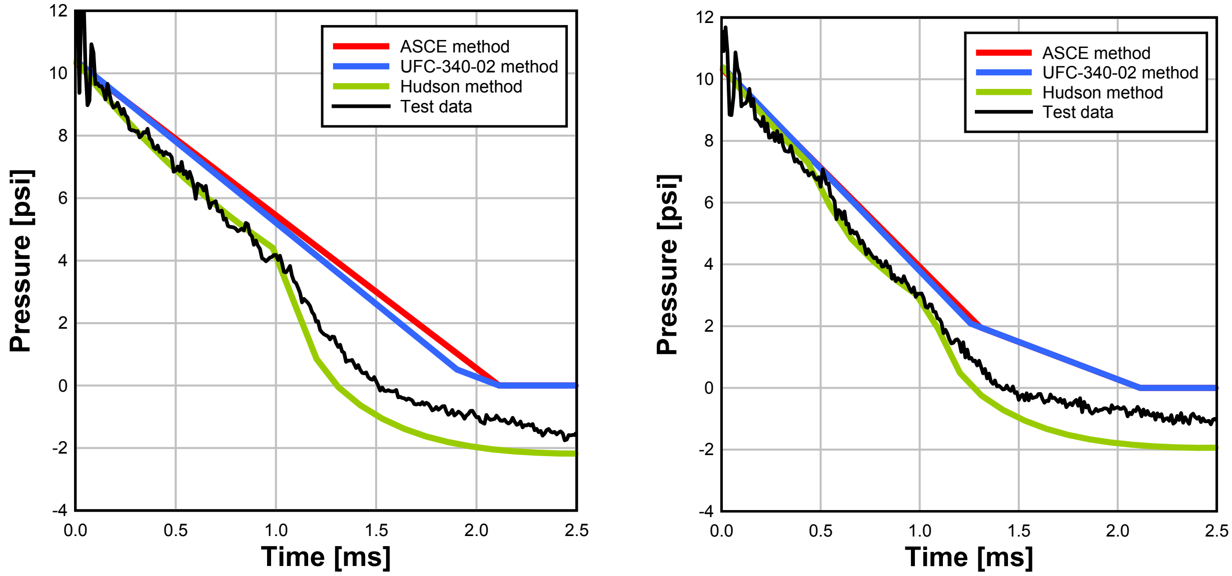

(a) G1 at centre **(b) G2 near top**

Figure 12: Comparison of test results to clearing methods for 4 m standoff.

At G2 nearer the top of the panel, the two manual methods agree and predict a clearing time of 1.2 ms. However, the test data shows the arrival of the first clearing wave from the top edge—and a departure from the smooth exponential decay—around 0.6 ms. A second clearing wave is clearly seen at 1.0 ms, which further decreases the pressure. Since this second wave is from the sides, it is not surprising that its arrival time is exactly the same as that seen earlier in G1. For this gauge also, Hudson predicts the arrivals of the various clearing waves with excellent accuracy. The first clearing wave (from the top, per Figure 9) has a magnitude that agrees well with the data, but the second (from the sides) is once again larger than the measured value.

At the standoff of 10 m the incident wave is longer, with a duration of around 3 ms (vs. 2 ms at a standoff of 4 m) as seen in Figure 13. The result at G1 shows a rather significant variability in the clearing time predicted by the two manual methods: 2.0 ms per UFC and 2.8 ms per ASCE. The Hudson waveform shows the clearing wave arriving at 1.0 ms, very much in keeping with the test data. The magnitude of decrease created by the clearing as predicted by Hudson agrees well with the test data at early times, but then drifts significantly lower for times beyond 1.5 ms. At G2, the two manual methods agree on the clearing time, but once again the Hudson method correctly predicts a much earlier arrival of the initial clearing wave, followed by a distinct second clearing wave due to the side edges. Hudson's arrival time predictions are excellent and the pressure magnitude after one clearing wave is brilliant, but when the second/third waves arrive the predicted pressure once again drifts low and diverges somewhat from the experimental result.

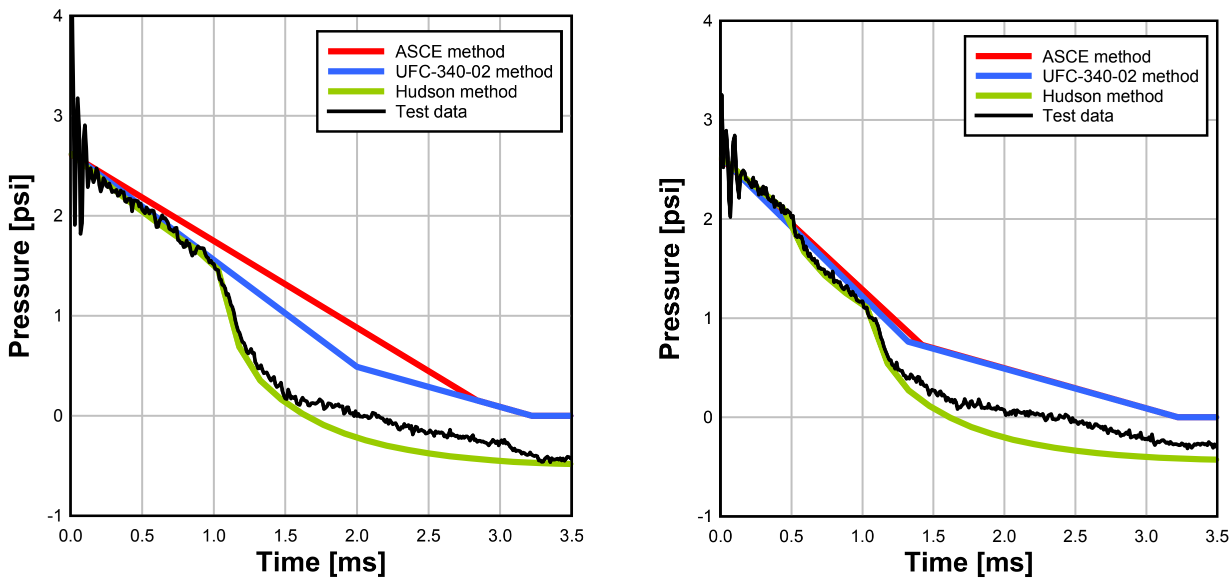

(a) G1 at centre **(b) G2 near top**

Figure 13: Comparison of test results to clearing methods for 10 m standoff.

Overall, Hudson's pressure history is very consistent with the early time data, but seems to diverge and underpredict pressure at later times. If we may generalise from this limited data set, arrival of a single wave seems to produce a highly realistic clearing wave, but superposition of multiple such waves seems to lead to an overprediction of clearing (and thus an underprediction of pressure). Nonetheless, in comparison to the manual methods, Hudson does a far better job in predicting the measured waveform and, most importantly, the overall reflected impulse, as will be discussed next.

Impulse

The primary reason for considering clearing effects is to more accurately predict impulse on the building. How then does the choice of clearing methodology affect impulse? In Table 1, we list the impulse for each gauge considered using all three prediction methods along with the actual test result. We then calculate the relative error in each method as:

$$E = \frac{I_{predicted} - I_{measured}}{I_{measured}} \tag{3}$$

Table 1: Maximum positive phase impulse values [psi-ms].

Standoff	Gauge	ASCE	UFC	Hudson	Test
4 m	G1	10.93	10.45	7.63	8.22
	G2	8.83	8.75	6.83	7.39
10 m	G1	3.96	3.42	2.39	2.56
	G2	3.03	2.97	2.14	2.36

A value of 0 would mean a perfect prediction, a positive value would mean an overprediction, and a negative value an underprediction. The relative error is plotted in Figure 14. Orange is used to for the 4 m test and purple for the 10 m; a circle is used for the centre gauge (G1) and a triangle for the top gauge (G2). Overall, both ASCE and UFC overpredict the impulse by a wide margin, 20-35 percent in seven of the eight cases, and 55% in the eighth. Oddly, the predictions are consistently better at G2 than at G1, even though we might expect the methods to have been empirically calibrated for a target at ground level.

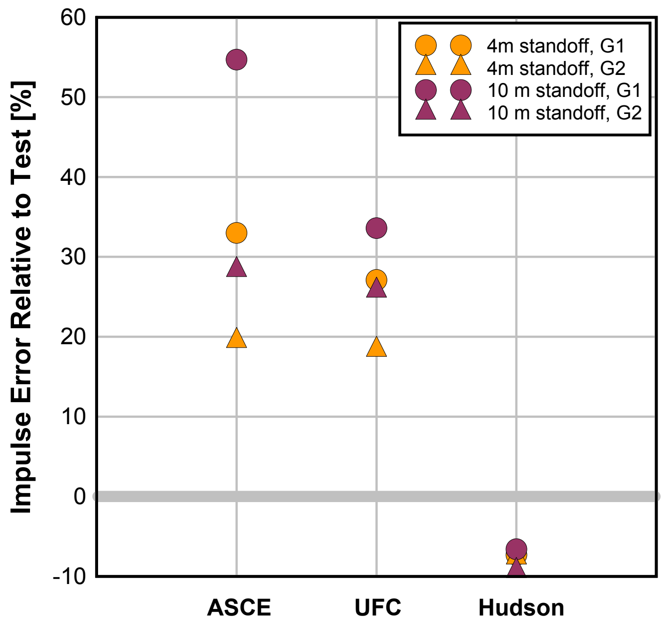

Figure 14: Relative error in impulse predictions from clearing methods.

The Hudson results are much closer to the test data, being 9% below the test in the worst case. The Hudson results show a modest negative bias relative to the data and a very small scatter. A plot of the average error for all the measurements is shown in Figure 15. Overall, ASCE overpredicts impulse by one-third, UFC by one-fourth, while Hudson underpredicts by one-twelfth.

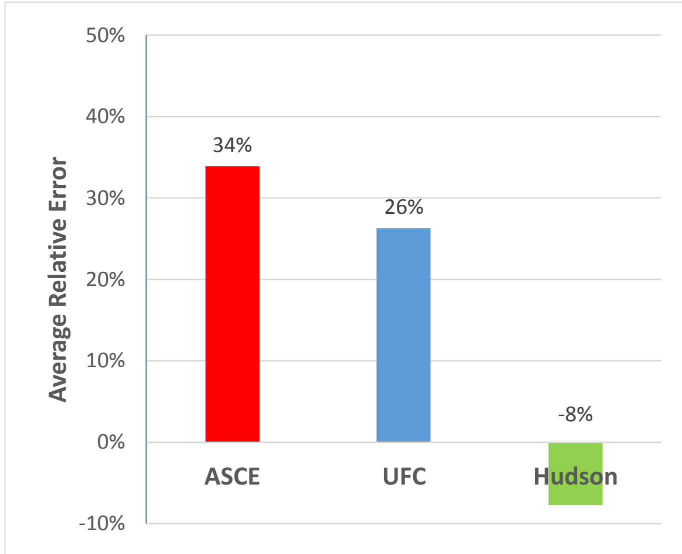

Figure 15: Average relative error for all gauges, all standoffs, for each prediction method.

CONCLUSIONS

From the preceding discussions and comparisons, it is evident that the Hudson approach provides a reliable, physical basis for deriving pressure histories that match well with data from controlled open-air blast tests. The method produces a lower relative error on impulse than the UFC or ASCE methods and accurately reproduces the details of the pressure measurements, including the scalloped shape of the waveform and the non-simultaneous arrival of clearing waves from different edges. It has the added advantage of being elegantly formulated in a single and relatively simple-to-use graph, with but one (equally simple) rule for exemption of clearing rays.

Nonetheless, it is fair to say that UFC/ASCE are design manuals with a view towards design conservatism rather than analytic fidelity, and that they are meant to apply to the total pressure on the entire wall rather than the pressure at a particular pinpoint target. As such, it is reassuring, particularly to those who use these manuals in their engineering practice, that both methods are conservative and lead to a higher applied impulse than would actually be expected.

Improvements in the Hudson method are clearly possible and worth pursuing. The method is consistently underpredicting impulse, and while the margin of this bias is small (8%), the fact that it is non-conservative will hinder its widespread adoption. Indications are that the method is more successful when applied to *single* clearing waves, but that it is overpredicting the magnitude of the relief wave when *multiple* clearing waves are simultaneously superimposed. Perhaps the assumption of linear superposition breaks down for such multiple waves. Further research that considers gauges at a more diverse set of locations should be able to illuminate this point and, if necessary, apply correction factors.

In the final analysis, whether this degree of refinement matters is a legitimate question. A photo of a building exposed to blast in a relatively recent bombing provides some clarification (Figure 16). It's quite clear that window breakage at this particular level of free-field loading is very closely correlated to distance from a free edge: windows along the top, sides, and bottom (since there was an overhang or set-back at the ground floor) experienced lower impulse, and survived. Windows near the centre had less benefit from clearing, experienced higher impulse, and failed.

Figure 16: Window damage in a building subjected to blast loads.

A counter-argument would be that no engineer would actually design the windows along the periphery of the façade to have thinner glazing than the windows in the centre, and that is surely a fair argument. In a design environment, use of a more conservative loading that ignores clearing altogether is practical and streamlines the design process. However, conditions will arise in which clearing must be considered, such as in the forensic analysis of the particular event illustrated in Figure 16, should the purpose of the analysis be to deduce the effective weight of the detonated device. Another relevant application would be for design of a wide, low building whose wall panels would all experience clearing from the top edge in a more-or-less consistent manner.

For these situations and others, we see tremendous potential in the Hudson method and would commend it to our colleagues as the most physically rigorous and accurate approach for accounting for clearing effects at a point on a reflecting surface. With further research and improvement, the method will only become more accurate and applicable over a wider domain of the parameter space.

REFERENCES

[1] C. Kingery and G. Bulmash, "Airblast Parameters from TNT Spherical Air Burst and Hemispherical Surface Burst," ARBRL-TR-02555, Ballistic Research Laboratory, 1984.

[2] "Structures to Resist the Effects of Accidental Explosions," U.S. Department of Defense, UFC 3-340-02, Change 2, September 2014.

[3] "Design of Blast Resistant Buildings in Petrochemical Facilities", 2nd Edition, Task Committee on Blast Resistant Design, American Society of Civil Engineers, 2010.

[4] D. Hyde, ConWep ver. 2.1.0.8, Geotechnical/Structures Laboratory, USAE Engineer Research & Development Center, Vicksburg, Mississippi.

[5] A. Tyas, J. Warren, T. Bennet, and S. Fay, “Prediction of clearing effects in far-field blast loading of finite targets,” Shock Waves (2011) 21:111-119.

[6] C.C. Hudson, “Sound pulse approximations to blast loading (with comments on transient drag)”. Technical Report SC-TM-191-55-51, Sandia Corporation, MD, USA, 1955.